Pharmaceutical Research, Vol. 22, No. 11, November 2005 (© 2005)
DOI: 10.1007/s11095-005-7626-9

Research Paper

Quantification of Crystallinity in Substantially Amorphous Materials by Synchrotron X-ray Powder Diffractometry

Cletus Nunes,[1,4] Arumugam Mahendrasingam,[2] and Raj Suryanarayanan[1,3,5]

Received May 19, 2005; accepted July 25, 2005

Purpose. The aim of this study was to develop a highly sensitive powder X-ray diffraction (XRD) technique for quantification of crystallinity in substantially amorphous pharmaceuticals, utilizing synchrotron radiation and a 2-D area detector.
Methods. Diffraction data were acquired at the European Synchrotron Radiation Facility (France) using a 2-D charge-coupled device detector. The crystallization of amorphous sucrose was monitored *in situ*, isothermally at several temperatures in the range of 90 to 160°C. An algorithm was developed for separation of the crystalline and amorphous intensities from the total diffraction pattern.
Results. The synchrotron XRD technique allowed powder diffraction patterns to be recorded with a time resolution of 40 ms. The gradual crystallization of sucrose is analogous to a series of physical mixtures with increasing content of the crystalline component. The *in situ* crystallization approach circumvented the problem of inhomogeneity in mixing—a potentially serious issue at extreme mixture compositions. The estimated limit of detection of crystalline sucrose in an amorphous matrix was 0.2% w/w, a considerable improvement over the reported value of ~1% w/w with a conventional XRD.
Conclusion. High-intensity XRD can discern *subtle* changes in the lattice order of materials. The first evidence of crystallization can serve as an indicator of the potential physical instability of the product.

KEY WORDS: amorphous; crystallinity; pharmaceuticals; synchrotron; X-ray diffraction.

INTRODUCTION

Amorphous materials have a higher free energy than their crystalline counterparts. Consequently, amorphous compounds have an increased tendency to undergo physical and chemical changes. Even so, the use of an amorphous ingredient in a formulation may be necessary to obtain a drug product with required biopharmaceutical properties. Amorphous materials often exhibit higher "apparent" solubility and faster dissolution rate than the corresponding crystalline materials. The apparent solubility of amorphous indomethacin, novobiocin, and tetracycline were 1.4, 10, and 2.5 times that of their respective crystalline counterparts (1–3). This increase in the apparent solubility can translate to increase in the oral bioavailability of drugs with poor aqueous solubility. In pharmaceutical products prepared by freeze-drying, the physical state of the active pharmaceutical ingredient (API) and excipients can influence product stability and performance. Lyoprotectants, i.e., additives added to stabilize proteins during freeze-drying and subsequent storage, must exist in an amorphous state to remain effective (4–6).

Because an amorphous → crystalline transition is thermodynamically favored, the use of amorphous material in dosage forms poses a challenge. Crystallization of an amorphous drug can occur even when it is stored below its glass transition temperature (T_g) (7). It is necessary to develop techniques to assess the rate and extent of crystallization. Very early detection of crystallization not only identifies physical instability, but may also permit corrective action. Moreover, an early detection of subtle changes in the solid state of the API in the drug product can be important from the viewpoint of ensuring therapeutic efficacy throughout the shelf life of the formulation (8–10).

Several analytical methods have been developed for quantification of crystallinity. When dealing with substantially amorphous materials, FT-Raman spectroscopy was shown to have high sensitivity (11). On the other hand, quantification techniques based on water sorption, calorimetry, and FT-Raman spectroscopy are reported to be of choice when dealing with highly crystalline substances having low levels of lattice disorder (11–14). Whereas X-ray diffractometry (XRD) is a widely used technique for quantification of the degree of crystallinity, the major limitation of conventional XRD is its low sensitivity, attributed mainly to the low flux of the X-ray source (12,15). Moreover, laboratory-based diffractometers generally use point detectors that scan through

[1] Department of Pharmaceutics, University of Minnesota, Minneapolis, Minnesota 55455, USA.
[2] Department of Physics, Keele University, Staffordshire, ST5 5BG, UK.
[3] 308 Harvard Street SE, 9-125 WDH, Minneapolis, Minnesota 55455, USA.
[4] Present address: Mylan Pharmaceuticals, Morgantown, West Virginia 26505, USA.
[5] To whom correspondence should be addressed. (e-mail: surya001@umn.edu)

the required 2θ angular range. Because it takes about 10–15 min for a typical X-ray run, rapid data acquisition is not possible. Preferred orientation can be a source of error in the peak intensity measurements. Another drawback is that the routinely used analytical procedures are somewhat subjective and prone to errors due to individual judgment (15).

CRYSTALLINITY QUANTIFICATION BY XRD

The procedure developed by Hermans and Weidinger for crystallinity quantification by XRD is most frequently used (16,17). The procedure is simple and based on three assumptions. First, it must be possible to demarcate and measure the crystalline intensity (I_c) and amorphous intensity (I_a) from the powder pattern. Second, there is a proportionality between the experimentally measured crystalline intensity and the crystalline fraction (x_c) in the sample. Finally, a proportionality exists between the experimentally measured amorphous intensity and the amorphous fraction (x_a) in the sample.

Thus,

$$x_c = pI_c \tag{1}$$

and

$$x_a = qI_a \tag{2}$$

where p and q are the proportionality constants.

The sum of amorphous and crystalline fractions is

$$x = x_c + x_a \tag{3}$$

Combining Eqs. (1), (2), and (3), we obtain

$$qI_a = x - pI_c \tag{4}$$

or

$$I_a = \left(\frac{x}{q}\right) - \left(\frac{p}{q}\right)I_c \tag{5}$$

The values of I_a and I_c can be determined for samples of varying degrees of crystallinity. A plot of the experimentally measured values of I_a against those of I_c should result in a straight line with a slope of p/q. The intercepts on the y and the x axes will provide the intensity values of the 100% amorphous and 100% crystalline materials, respectively.

The degree of crystallinity, x_{cr} (expressed as a percentage), of a sample is given by

$$x_{cr} = \frac{x_c}{x_c + x_a} \times 100 \tag{6}$$

or

$$x_{cr} = \frac{I_c}{I_c + \frac{q}{p}I_a} \times 100 \tag{7}$$

Thus, to calculate percent crystallinity values using Eq. (7), (i) the I_c and I_a values need to be separated from the total X-ray pattern and (ii) the value of the proportionality constant, q/p, should be known.

Limitations of the Procedure

(i) The demarcation of the crystalline (I_c) and amorphous (I_a) intensities from the experimentally obtained X-ray diffraction pattern is done arbitrarily and is subject to individual judgment. The procedure may thus lead to high variability in the results, especially when the degree of crystallinity is low.

(ii) Samples may show preferred orientation effects, which may cause significant errors in peak intensity measurement. An effective way to minimize preferred orientation is to decrease the particle size of the sample by grinding. However, the grinding process itself can cause undesired changes in the solid state of the material.

(iii) It is necessary to generate a standard curve using samples with different degrees of crystallinity. A common procedure is to mix crystalline and amorphous standard phases in appropriate proportions. Nonhomogenous mixing becomes a potentially important issue, especially when preparing mixtures of extreme compositions.

Our investigation had two objectives: (i) to develop an X-ray diffractometric technique, based on synchrotron X-rays and a 2-D area detector, having increased *sensitivity* and *rapid data acquisition capability* compared to conventional instruments and (ii) to develop an *objective* method for calculating the degree of crystallinity based on an algorithm. The key analytical challenge, from a pharmaceutical perspective, has been to develop a technique capable of discerning *subtle* changes in lattice order in substantially amorphous materials. Our focus was therefore on the detection and quantification of the first evidence of crystallization in an amorphous material. An *in situ* crystallization approach was used to overcome the problem of inhomogeneity in mixing, which is a particularly serious issue at extreme mixture compositions.

Sucrose was selected as the model compound based on its following attributes (12,18–20): (i) Sucrose can be readily rendered amorphous by freeze-drying. (ii) Heating of amorphous sucrose above its glass transition temperature of 74°C causes its complete crystallization. (iii) There are no issues of polymorphism or solvate formation in sucrose.

MATERIALS AND METHODS

Materials

Preparation of Amorphous Sucrose

Sucrose was obtained from Mallinckrodt Baker Inc. (Paris, KY, USA). Aqueous sucrose solutions (10% w/v, filtered through 0.2-μm membrane filter) were cooled from 25 to −50°C at 1°C/min in a tray freeze-dryer (Advantage 2.0 ES, Virtis, NY, USA), and held for 3 h. The chamber pressure was then set to 50 mTorr. Primary drying was carried out at −40°C for 48 h. Thereafter, the shelf temperature was increased up to 40°C at 1°C/min, with an isothermal hold for 10 h at 5°C intervals. The samples were stored in a vacuum desiccator at room temperature.

Preparation of Crystalline Sucrose

Amorphous sucrose was annealed at 130°C for ~15 min. The powder X-ray pattern indicated that the sample was highly crystalline. Water sorption experiments in an automated vapor sorption apparatus (DVS-1000, Surface Measurement Systems, London, UK) did not reveal detectable weight gain over the relative humidity (RH) range of 5 to 35%, indicating that the sample was completely crystalline (12,21,22).

Methods

Baseline Characterization

Powder XRD. The sample was placed in an aluminum holder by the side-drift method and was exposed to CuKα radiation (45 kV × 40 mA) in a wide-angle X-ray powder diffractometer (Model D5005, Siemens, Munich, Germany). The instrument was operated in a step scan mode, in increments of 0.05° 2θ. The angular range was 5 to 40° 2θ, and counts were accumulated for 1 s at each step.

Differential Scanning Calorimetry (DSC). A differential scanning calorimeter (Model 2920, TA Instruments, New Castle, DE, USA) equipped with a refrigerated cooling accessory was used. The instrument was calibrated with pure samples of tin and indium. About 4–5 mg sample was packed in aluminum pans, crimped nonhermetically, and heated at 10°C/min under dry nitrogen purge from room temperature to 200°C.

Thermogravimetric Analysis (TGA). The sample was heated in an open aluminum pan from room temperature to 200°C, under nitrogen purge, at 10°C/min in a thermogravimetric analyzer (Q50, TA Instruments).

Water Vapor Sorption. About 15 mg of sample was placed in the sample pan of an automated vapor sorption balance (DVS 1000, Surface Measurement Systems) and dried at ~0% RH under dry nitrogen purge (flow rate of 200 ml/min) for 12 h. Thereafter, the RH of the sample chamber was progressively increased to 35% over a period of 24 h. The sample weight change was monitored as a function of time. The experiments were conducted at 25°C.

Sample Preparation for XRD in Transmission Geometry

In XRD using transmission geometry, the incident X-ray beam passes through the sample and the diffraction pattern is acquired using a 2-D area detector positioned on the opposite side of the sample (in relation to the X-ray source). The "vertical" configuration of "powder" samples was made possible by filling sucrose samples (~20 mg) in aluminum pans (used generally for differential scanning calorimetry, TA Instruments), and the pans were crimped nonhermetically. The sample preparation (weighing, filling, and crimping) was performed in a glove box maintained at RH <1% by a continuous purge of dry nitrogen gas.

2-D XRD Using a Rotating Anode X-ray Generator

X-rays were generated with a rotating copper anode (Model RU-200BVH, Rigaku, Tokyo, Japan) operated between 2.5 and 6 kW power. The diffractometer was set up in the transmission geometry and used "Franks mirror" optics to yield a ~200-μm-diameter beam on the sample. The focusing optics produce an X-ray beam of much higher intensity than that obtained with pinhole collimators. The sample chamber consisted of a 7 × 15 × 20 cm enclosure having polyimide film (Kapton, DuPont, Wilmington, DE, USA) covered windows for the entry and exit of the incident and diffracted X-ray beams, respectively. The chamber was contained in a sample stage fitted with cartridge heaters connected to a water/glycol-based cooling system. The temperature of the stage could be adjusted and controlled within 1°C, using a temperature controller (CN8500, Omega Instruments, Stamford, CT, USA) interfaced with a PC via Labview (National Instruments, Austin, TX). The chamber was purged with dry helium during experiments. The 2-D diffraction patterns were collected using a multiwire area detector (HISTAR, Bruker, WI, USA). The sample (~20 mg), filled in a crimped (DSC) pan, was placed on the sample stage and a powder pattern was recorded at room temperature. The sample was then removed from the stage, the stage heated to the desired temperature, and the sample reinserted into the chamber. Diffraction data were obtained with a 30-s integration time per pattern. Crystallization of amorphous sucrose was studied isothermally at several temperatures in the range of 90 to 110°C. At the end of each experiment, the sample stage was heated to 160°C and an X-ray pattern was obtained to confirm the complete crystallization of sucrose.

Time-Resolved 2-D XRD Using Synchrotron Radiation

Experiments were performed on the ID-2 beamline at the European Synchrotron Radiation Facility (ESRF, Grenoble, France). The beamline, equipped with an undulator, provided a highly collimated [~70 × 25 μrad^2 (horizontal × vertical) divergence] and intense beam (~10^{13} photons s^{-1} $mrad^{-2}$ per 0.1% bandwidth). A monochromatic [$(\Delta\lambda/\lambda) = 2 \times 10^{-4}$] X-ray beam of 0.995 Å wavelength was selected using a cryogenically cooled Si(111) double-crystal monochromator. The experiments were preformed in the transmission mode. The incident beam size at the sample was adjusted to 50 × 75 μm. Calibration was performed using Al_2O_3 standard (SRM 674a, NIST). The sample chamber was a 15 × 15 × 15-cm enclosure containing two electrical heating elements and two air-circulating fans. The temperature could be controlled to within 1°C, and the maximum attainable temperature was 350°C (23). The sample chamber was fitted with a horizontal bar driven by a computer-controlled stepper motor and an electronic trigger. The horizontal bar contained a small cavity at its end for vertical placement of the aluminum sample pan. A 2-D charge-coupled device detector (Photonic Science, East Sussex, UK) was used for acquiring the diffraction data.

At the start of each experiment, the sample (~20 mg) sealed in an aluminum pan, was placed vertically on the horizontal bar (maintained at room temperature) of the sample chamber. The main sample chamber was preheated to the desired temperature. The sample mounted on the horizontal bar was inserted into the preheated sample chamber by activation of the trigger, thus exposing the sample to the incident X-ray beam. The sample was rapidly oscillated about its

mean position by using a stepper motor connected to the horizontal bar. Diffraction data were obtained continuously as snapshots with a time resolution of 40 ms, in the transmission geometry, as the sample was held under isothermal conditions. The data were digitized by a Synoptic i860 frame grabber in an 8-bit word binary data format. The details of the setup have been described in detail elsewhere (24–26). The signal-to-noise ratio was improved by integrating successive frames together. The integration time for each successive powder diffraction pattern was adjusted between 0.5 and 3 s, taking into account the reaction rate and the memory capacity of the frame grabber. The crystallization of amorphous sucrose was studied isothermally at several temperatures in the range of 110 to 160°C. At the end of each experiment, the sample chamber was heated to 160°C, and an X-ray pattern was obtained to confirm the complete crystallization of sucrose.

Algorithm for Separation of I_a and I_c from an X-ray Pattern

Our goal was to develop an objective method to separate the crystalline and amorphous intensity components from an X-ray pattern. Each 2-D XRD pattern is composed of an intensity signal arranged on a grid of 512 × 512 pixels. Because synchrotron-based XRD experiments generated enormous amount of diffraction data (time resolution of 40 ms, integration time of 0.5 to 2 s), software routines (macros) were developed for data analysis. The analyses were performed on a UNIX and LINUX platform. The key steps involved in analysis of diffraction patterns were as follows.

(i) Each 2-D X-ray pattern was first corrected for the spatial distortion profile of the detector using a calibration grid (27). The center coordinates for the diffraction pattern (Debye rings) were determined, and the 2-D data were converted from the Cartesian to a polar coordinate system. (ii) An algorithm was developed that subdivided the diffraction pattern into small "probe" sectors of a predetermined size. A smoothing kernel (four points) was used to minimize random electronic noise in the recorded data. The minimum intensity signals in each sector were determined, and the results were stored in a separate data file. The operation was performed successively for all the probe sectors. (iii) Subsequently, the probe sectors were redrawn such that the boundaries were translated by one pixel in the x and y directions with respect to the former step. The process of assigning sectors and subsequent computation steps was repeated successively until all diffraction data were analyzed. (iv) A 2-D surface was generated by using the intensity signal data generated by the above algorithm. The surface thus generated describes the intensity contribution due to the amorphous component. The subtraction of the amorphous intensity from the total pattern yields the crystalline component. (v) Summation of the amorphous and the crystalline patterns provide the values of I_a and the I_c, respectively. The operation was checked for robustness by varying the sector sizes and translation areas. (vi) The instrument background signal (due to air, incoherent scattering, sample pan) was extracted using the X-ray pattern of the completely crystalline material obtained at the end of each *in situ* crystallization experiment.

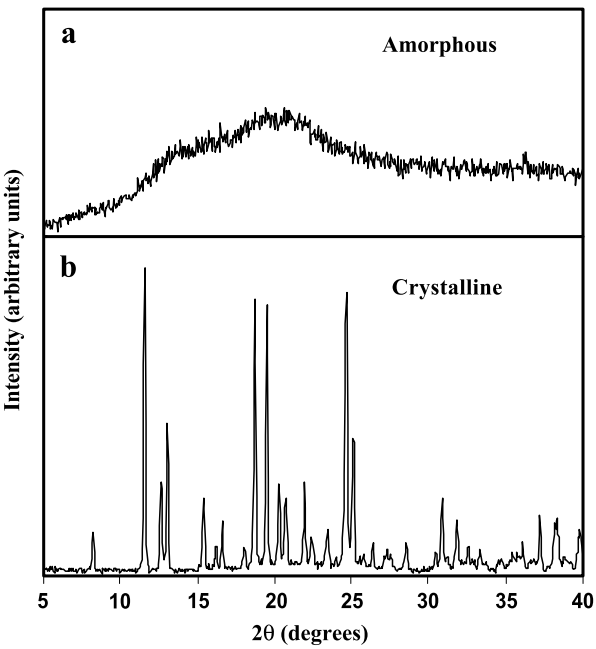

Fig. 1. Powder X-ray patterns of (a) amorphous, and (b) crystalline sucrose.

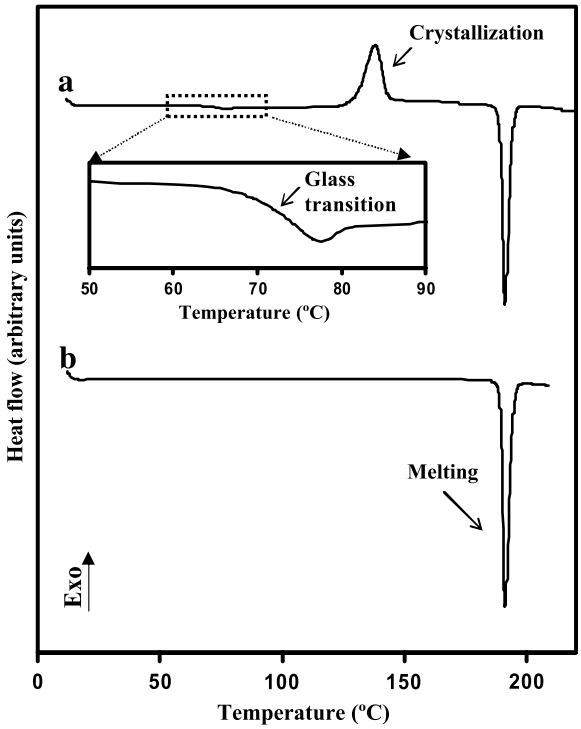

Fig. 2. DSC curves of (a) amorphous and (b) crystalline sucrose. The inset is an expanded DSC profile of amorphous sucrose in the temperature range of 50 to 90°C.

RESULTS AND DISCUSSION

Baseline Characterization of Amorphous and Crystalline Sucrose

The XRD pattern of amorphous sucrose showed a broad "halo" in the range of 7 to 30° 2θ (Fig. 1). The DSC curve showed a glass transition event at ~74°C, a crystallization

exotherm at ~138°C, and melting (endotherm at 190°C) of crystalline sucrose (Fig. 2). When subjected to TGA, a weight loss of <0.1% was observed in the temperature range of 25 to 125°C, indicating that amorphous sucrose, which was stored under dry conditions, had very little sorbed water (results not shown). The amorphous sucrose was considered to be completely amorphous, i.e., 0% crystalline.

The X-ray pattern of crystalline sucrose (Fig. 1) consisted of sharp peaks and was in excellent agreement with the pattern reported in the Powder Diffraction Files maintained by the International Centre for Diffraction Data (28). The DSC curve revealed a single endotherm attributed to melting at 190°C (Fig. 2). The TGA curve did not reveal any detectable weight loss in the temperature range of 25 to 190°C. Crystalline sucrose did not sorb water when exposed to progressively increasing RH up to 30% for 3 days in an automated water sorption apparatus. Amorphous materials, including amorphous sucrose, have a strong tendency to sorb water (12,29–31). Thus, the XRD, DSC, TGA, and water sorption experiments showed that the sample is completely crystalline, i.e., 100% crystalline.

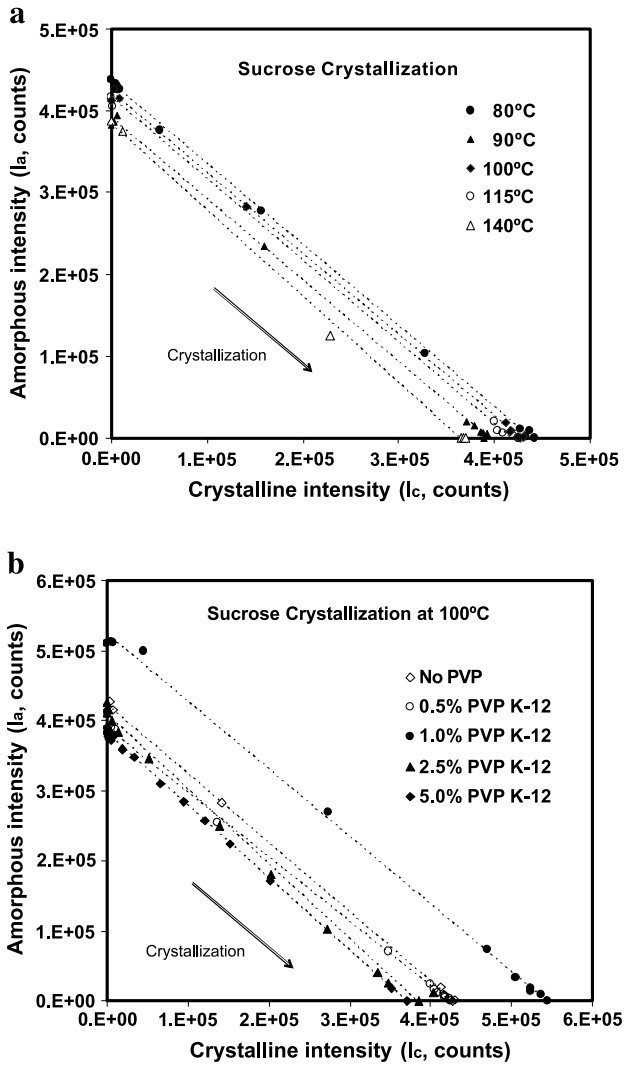

Fig. 3. (a) Plot of amorphous (I_a) *vs.* crystalline (I_c) intensity during the isothermal crystallization of amorphous sucrose. The slope of the regression lines (dashed lines) provided the value of the proportionality constant, q/p [Eq. (5); results presented in Table I]. The experiments were performed on a rotating anode X-ray diffractometer. Because the crystallization was rapid (<8 min), only a few diffraction patterns could be obtained. (b) Plot of amorphous (I_a) *vs.* crystalline (I_c) intensity during the isothermal crystallization of amorphous sucrose at 100°C. PVP (grade K-12) was used as an additive.

Table I. Values of q/p for Sucrose Crystallization Determined from the Plot of Amorphous (I_a) *vs.* Crystalline (I_c) Intensities [Eq. (5)]

Temperature of crystallization (°C)	Additive (PVP) Grade	Conc. (% w/w)	q/p	Mean	SD	CV (%)
80	–	0.0	1.009			
90	–	0.0	1.005			
100	–	0.0	1.011	0.995	0.027	2.7
115	–	0.0	1.001			
140	–	0.0	0.948			
100	–	0.0	1.011			
100	K-12	0.5	1.086			
100	K-12	1.0	1.041			
100	K-12	2.5	0.935	1.001	0.048	4.8
100	K-12	5.0	0.964			
100	K-25	0.5	1.020			
100	K-25	1.0	0.970			
100	K-25	2.5	0.983			

Experiments performed on a rotating anode diffractometer.

Computation of the Value of the Proportionality Constant, q/p

The objective of this study was to develop an XRD technique capable of discerning the first evidence of crystallization of an amorphous material [Eq. (7)]. A usual approach is to generate a standard curve using binary mixtures of crystalline and amorphous sucrose of various compositions. However, when dealing with solids, the errors due to inhomogenous mixing can become significant, especially when the analyte concentration is low. This problem becomes accentuated when dealing with amorphous and crystalline materials because these two phases often have a large difference in their bulk densities (32). Therefore, we used an alternative approach wherein amorphous sucrose was allowed to crystallize *in situ* under isothermal conditions in the X-ray sample chamber. The rapid transition of sucrose from a completely amorphous (assumed to be 0% crystalline or 100% amorphous) state to a completely crystalline (assumed to be 100% crystalline or 0% amorphous) state was monitored by acquiring 2-D X-ray diffraction data, as snapshots, during the entire crystallization event.

As described in the "Introduction," the degree of crystallinity (or percent crystallinity) is defined by Eq. (7). However, a simpler expression, the term "crystallinity index," is expressed as follows (33,34).

$$\text{Crystallinity index}(\%) = \frac{\text{Intensity of crystalline peak}(s) \times 100}{\text{Total diffracted intensity}} = \frac{I_c \times 100}{I_c + I_a} \quad (8)$$

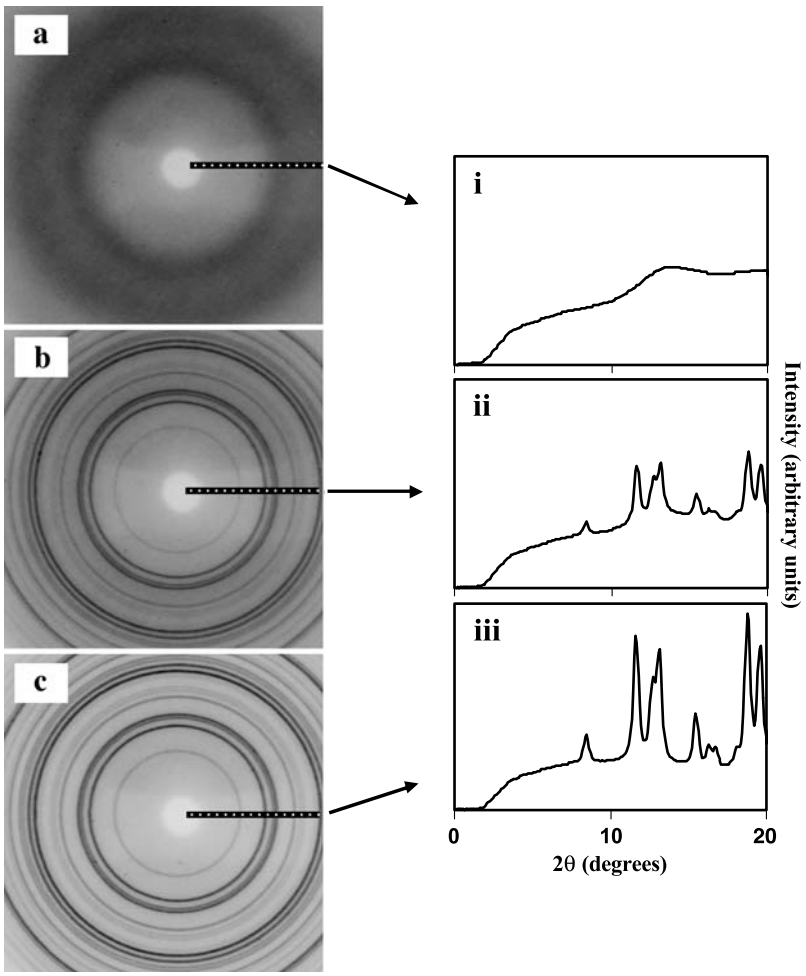

Fig. 4. 2-D X-ray patterns of (a) amorphous, (b) partially crystalline, and (c) crystalline sucrose. Darker shade represents higher intensity. Inner rings represent lower 2θ values. Patterns are corrected for detector distortion effects. Instrument background has not been removed. To facilitate visualization, the diffraction data are presented in one dimension as "intensity *vs.* 2θ" plots (i, ii, and iii).

The crystallinity index (%) is numerically equal to the "percent crystallinity" (Eq. 7) if q/p is equal to 1.

The Hermans and Weidinger procedure [Eq. (7)] assumes that the sample packing and the irradiated volume are maintained constant during the entire set of experiments. Any sample-to-sample variation in irradiated volume will affect the magnitude of q/p [slope of the I_a *vs.* I_c plot, Eq. (5)] and can lead to erroneous results. When the XRD experiments are conducted in the transmission mode, the diffracted intensity can be influenced by the sample packing and powder bed thickness. However, if the magnitude of q/p is demonstrated to be close to unity, then Eq. (7) reduces to Eq. (8). The results will not be sensitive to small changes in sample packing and the crystallinity index $\cong$ percent crystallinity.

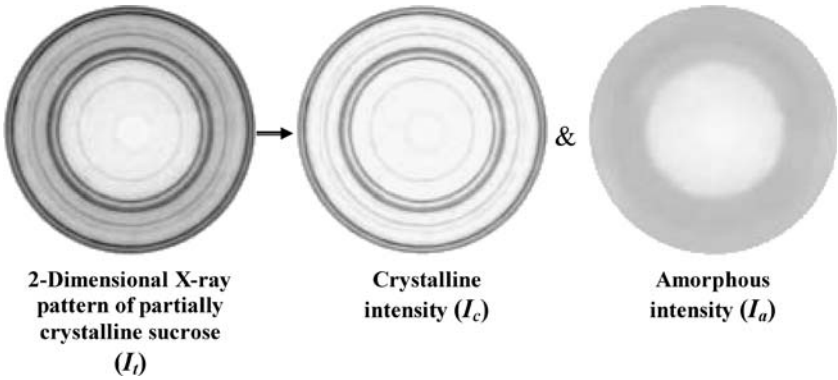

Fig. 5. Separation of the 2-D X-ray patterns of partially crystalline sucrose into crystalline (I_c) and amorphous (I_a) intensity components.

Our goal therefore was to determine the value of the proportionality constant, q/p, for sucrose. Aluminum pans were tightly filled with the amorphous sucrose samples and nonhermetically sealed. The isothermal crystallization was monitored using a rotating anode X-ray source and an area detector. The X-ray patterns were collected at 30-s intervals. The crystalline (I_c) and amorphous (I_a) components of the X-ray patterns were separated and I_a was plotted as a function of I_c (Fig. 3a). In an effort to decelerate analyte crystallization, sucrose was lyophilized with polyvinylpyrrolidone (PVP, a crystallization inhibitor) (35). This approach enabled us to collect more data points during the crystallization experiment (Fig. 3b). The plots revealed that the slope values [i.e., q/p, Eq. (5)] of the regression lines were very close to unity (Table I). The x and y intercepts of the individual plots were different due to the small run-to-run differences in the volume of the sample packed in the holder. The major drawback of the rotating anode setup was the limited time resolution and sensitivity. This experimental setup was unsuitable for detecting subtle changes in crystallinity because only a limited number of data points can be collected. A high-intensity synchrotron source does not have these limitations.

Crystallinity Quantification Using Synchrotron XRD

As mentioned earlier, we were specifically interested in developing a 2-D XRD technique for discerning the first evidence of crystallization of an amorphous material. The 2-D X-ray pattern of completely amorphous sucrose contained broad halos and absence of any crystalline Bragg reflections (Fig. 4a). As sucrose crystallized, the amorphous halo receded and crystalline reflections (Debye rings) appeared (Fig. 4b). Finally, the X-ray pattern of completely crystalline sucrose consisted of sharp crystalline rings (Fig. 4c). Further annealing of this sample did not cause any change in the X-ray pattern. Moreover, an identically annealed sample did

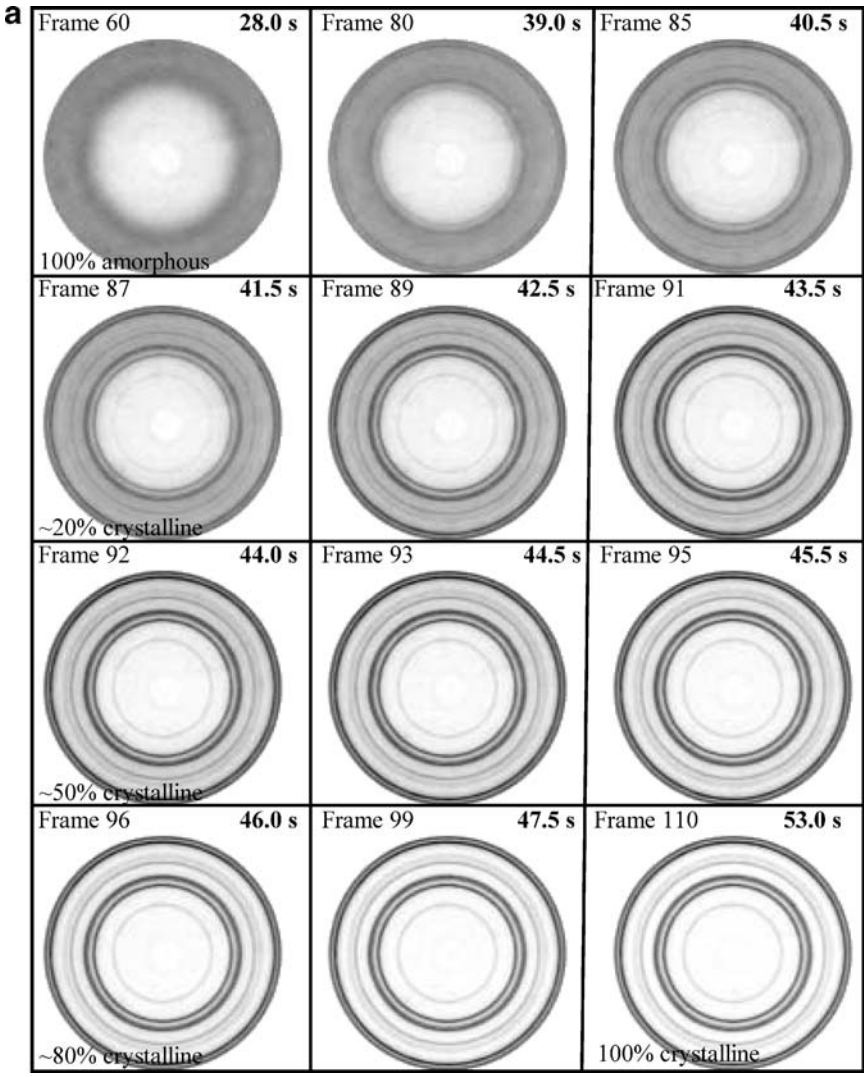

Fig. 6. (a) Powder X-ray patterns, i.e., total diffracted intensity (I_t) recorded during crystallization of amorphous sucrose at 150°C. The diffraction data for each 2-D pattern ("frame") were collected for 1/2 s. Only selected X-ray patterns are shown. (b) Crystalline intensity (I_c) separated from the total X-ray patterns (I_t, a). (c) Amorphous intensity (I_a) separated from the total X-ray patterns (I_t, a). Experiments performed on the synchrotron beamline.

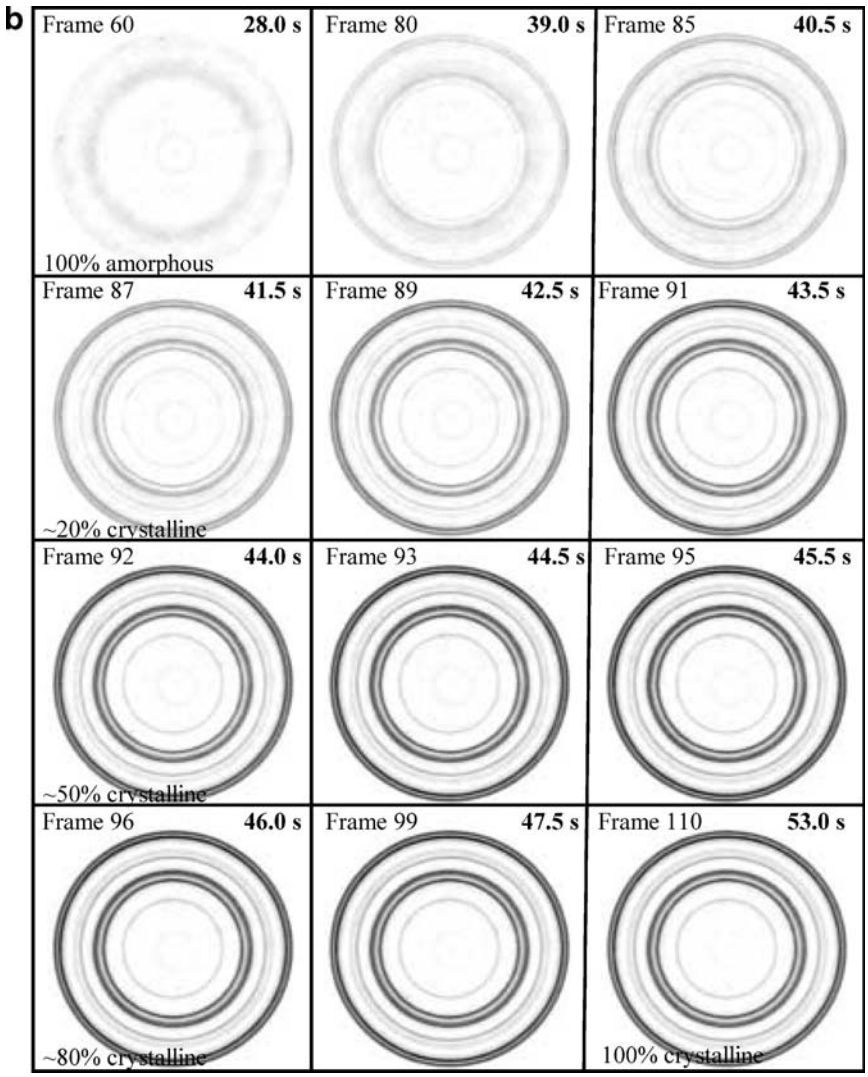

Fig. 6. Continued.

not show detectable water uptake in an automated water sorption apparatus at 10, 15, and 35% RH. These results show that sucrose crystallizes completely under the isothermal experimental conditions.

Separation of Amorphous and Crystalline Intensity Components

As described earlier and quantitatively described by Eq. (7), the X-ray pattern of a partially crystalline material has intensity contribution due to the crystalline (I_c) and the amorphous (I_a) fractions. To quantify the crystallinity, it is necessary to separate these two intensity contributions. We developed an algorithm, described in the "Materials and methods" section, to achieve this objective.

As a representative example, an X-ray pattern of partially crystalline sucrose is shown in Fig. 5. The "Bragg reflections" appear as concentric Debye rings. The center coordinates of the Debye rings were determined and the intensity data were transformed from the Cartesian to a polar coordinate system. Using the algorithm, the pattern was divided into "probe" sectors and processed to separate the crystalline (I_c) and amorphous (I_a) intensity components. Figure 5 shows the result of one such separation procedure.

The separation algorithm was used on all the successive X-ray patterns (frames) recorded during isothermal crystallization of sucrose, thereby spanning the entire crystallinity range, i.e., from 0 to 100% crystallinity. A representative series of diffraction patterns recorded during sucrose crystallization is shown in Fig. 6a. The corresponding separated crystalline and amorphous components of the patterns are shown in Fig. 6b and c, respectively. Integration of the intensities of the separated patterns provides the values of I_c and I_a.

Quantification of Subtle Changes in the Lattice Order of Sucrose During Crystallization

After carrying out the crystallization experiments at several temperatures, the q/p ratio was obtained by plotting I_c *vs.* I_a. The plots were constructed using the entire powder pattern. Similar plots were also constructed based on the intensity of a single (100) reflection. The q/p values obtained

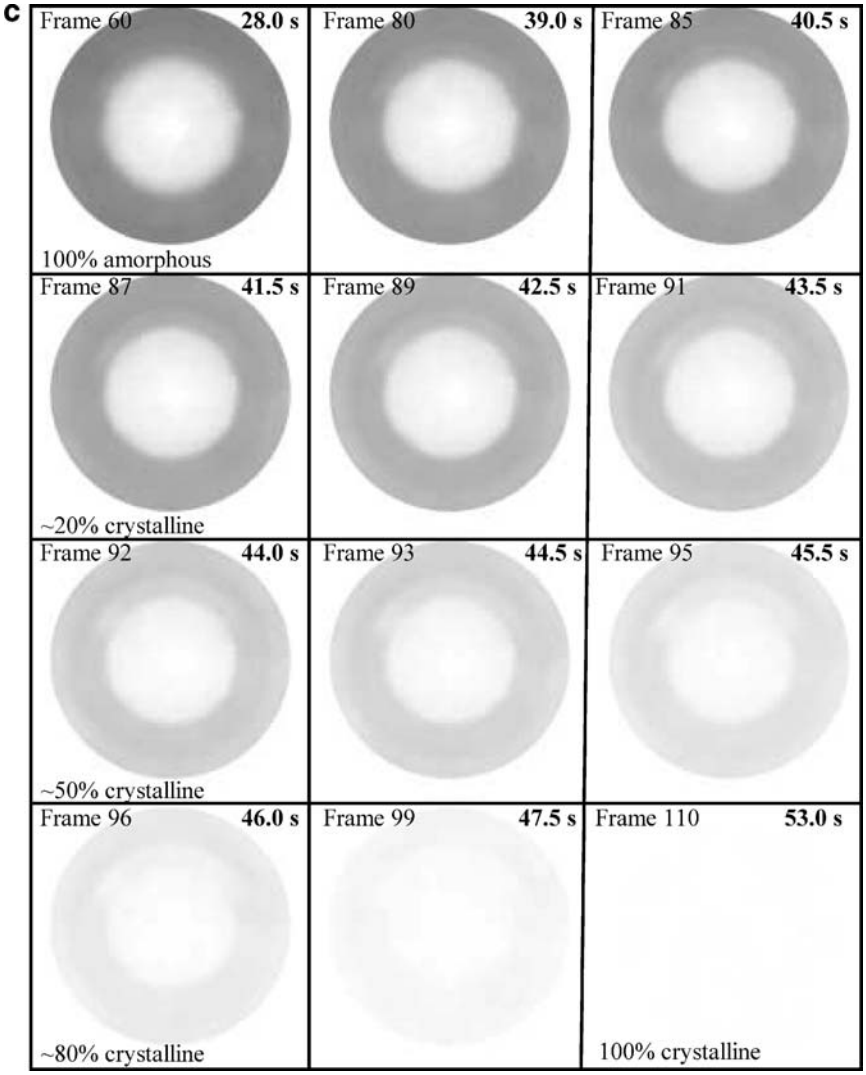

Fig. 6. Continued.

by the two methods were, in general, in good agreement and close to unity (Table II). These results indicated that the preferred orientation effects in the 2-D XRD method were minimal. There was also some within-run variation in the sample volume exposed to the synchrotron beam. The variation was attributed to (i) the powder flow, especially before the onset of crystallization when amorphous sucrose is heated rapidly to temperatures above its glass transition temperature, and (ii) to oscillation of the sample holder. As mentioned earlier, because $q/p \approx 1$, the results are independent of the irradiated volume and the "crystallinity index" ≈ "% crystallinity" [Eqs. (7) and (8)].

Figure 7a is a plot of the crystallinity index as a function of time, for sucrose crystallization at 150°C. It is noteworthy that even subtle changes (<0.2%) in lattice order at the early stages of crystallization could be detected and quantified (Fig. 7b, c). Similar results were obtained when the crystallization experiments were carried out at several other temperatures (data not shown).

From a pharmaceutical formulation perspective, early detection of crystallization can be crucial. The first evidence of crystallization suggests that adequate nucleation and growth has occurred. This could serve as an early indicator of the potential physical instability (amorphous → crystalline transition) of the product. Furthermore, trace amounts of small crystallites can serve as seeds and accelerate crystallization of the amorphous material during pharmaceutical processing and storage. As mentioned in the "Introduction", several analytical methods have been developed to quantify the degree of crystallinity of pharmaceuticals. However, the percent crystallinity values obtained by different analytical techniques often show poor agreement. Hence, too much emphasis should not be given to the absolute values of percent crystallinity. Nevertheless, the crystallinity estimates provide useful indication of the *relative* state of order of a material, and the data can be correlated with other properties of the solid that can influence product performance. Careful evaluation of the impact of subtle changes in the state of order can yield information useful toward developing a robust formulation. In our synchrotron-based experiments, although adequate attention was paid toward the characterization of both amorphous sucrose (DSC, TGA, X-ray powder pattern on conventional and high-intensity source) and crystalline sucrose (water sorption, DSC, XRD), it is best to consider the

Table II. The Values of "q/p" for Sucrose Crystallization Determined from the Plot of Amorphous (I_a) *Versus* Crystalline (I_c) Intensities [Eq. (5)]

	q/p	
Temperature of crystallization (°C)	Single peak [(100) reflection]	Entire powder pattern
150	0.990	0.983
150	1.042	1.020
150	1.042	1.064
160	0.990	0.980
160	0.978	0.963
160	1.053	1.031
170	0.980	0.971
Mean	1.011	1.002
SD	0.033	0.037
CV (%)	3.257	3.713

Experiments performed on a synchrotron XRD beamline.

development of crystallinity (0% crystalline → 100% crystalline) on a relative rather than an absolute scale. The data analysis procedures used yield results with a high degree of self-consistency and indicate that the technique is capable of discerning subtle changes in the state of order.

Estimate of the Limit of Detection

The gradual crystallization of amorphous sucrose is analogous to a series of physical mixtures prepared with increasing fraction of crystalline component. Thus, the *in situ* crystallization approach circumvented the problems associated with preparing solid mixtures containing low levels of analyte and allowed us to control the experimental variables.

In conventional validation procedures using standard mixtures of crystalline (analyte) and amorphous phases, the limit of detection (LOD) is given by the following equation (36):

$$\mathrm{LOD} = \frac{3 \times s_{\mathrm{blank}}}{m} \tag{9}$$

where s_{blank} is the standard deviation of "blank" signal and m is the slope of the standard curve.

The standard curve is obtained experimentally by plotting the "response signal" *vs.* "analyte composition" in the standard mixtures. However, for *in situ* crystallization processes, such a standard curve cannot be obtained. Hence,

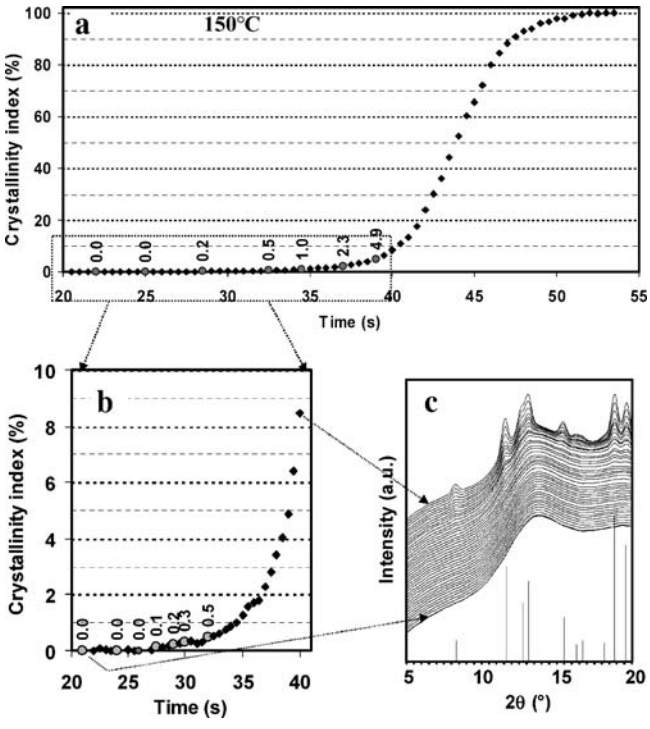

Fig. 7. (a) Plot of crystallinity index *vs.* time during crystallization of sucrose at 150°C. (b) Profile during the onset of crystallization. The percent crystallinity values at selected data points are indicated. (c) 1-D powder patterns (intensity *vs.* 2θ) at the early stages of crystallization. The stick patterns show the positions of the Bragg peaks of crystalline sucrose.

Table III. Estimated Limit of Detection for the Synchrotron XRD Technique

Temperature of crystallization (°C)	Slope (m) of the response signal (I_c, counts) *vs.* crystallinity (% w/w) plot [counts (% w/w)$^{-1}$]	Standard deviation of the blank signal $(I_c)_0\ s_{\mathrm{blank}}$	Limit of detection = $(3 \times s_{\mathrm{blank}})/m$ (% w/w)
140	21,502	1322	0.18
150	22,869	1224	0.16
150	22,853	1616	0.17
150	22,903	1075	0.14
160	21,407	1133	0.16
160	17,409	837	0.14
160	19,789	1196	0.18
Mean			0.16
SD			0.02
CV (%)			10.4

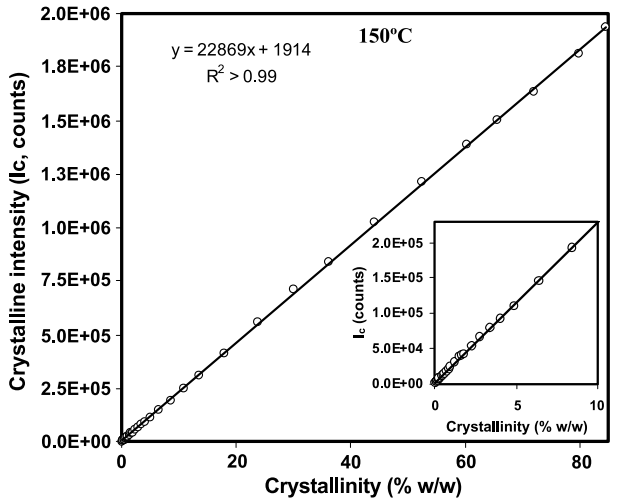

Fig. 8. Plot of crystalline intensity signal (I_c) *vs.* percent crystallinity. The temperature of crystallization was 150°C, and X-ray patterns were recorded with an exposure time of 0.5 s per pattern. The inset is an expansion of the plot corresponding to the region of <10% crystallinity.

the value for LOD, as defined in Eq. (9), cannot be determined. Nevertheless, an estimate of the LOD can be obtained (37) by plotting the "intensity response" against "crystallinity" (i.e., as amorphous sucrose is converted to a crystalline state). Figure 8 shows such a response signal *vs.* crystallinity plot. The large slope (m) value of the regression line indicates that the method is very *sensitive* to subtle changes in crystallinity. The slope of this curve can also yield an estimate of LOD using Eq. (9) (37). The standard deviation (s_{blank}) of the blank signal $(I_c)_0$ was determined by using data points obtained before the onset of crystallization (i.e., completely amorphous sample). The average estimated LOD thus obtained (Table III) was ~0.2% w/w crystalline content and was in good agreement with the experimental observations.

SIGNIFICANCE

The method developed is capable of revealing the first evidence of crystallization in an amorphous material. The estimated LOD of 0.2% w/w is a considerable improvement over the recently reported LOD of 0.9% w/w using conventional XRD (18). An important feature of the developed method is that the crystallinity quantification procedure is objective. Conventionally, the separation of the amorphous and the crystalline intensities is done arbitrarily and is subject to individual judgment. Such an analysis can lead to a high variability in results, especially when the weight fraction of the analyte (i.e., crystalline content) is low. From a pharmaceutical perspective, the early detection of crystallization in a formulation can be crucial. If crystallization is not desired, early information on the onset of crystallization can provide an opportunity to take appropriate corrective actions. These include (i) reassessment of the shelf life recommended for the product, and (ii) altering the storage conditions (e.g., decreased temperature or water vapor pressure). It is also likely that the stability of the amorphous material is compromised during pharmaceutical processing (e.g., exposure to water vapor, interaction with excipients containing water, or an increase in temperature during milling). A reevaluation of the processing operations may be warranted for ensuring product stability. Because XRD enables study of crystallization in complex matrices, the annealing technique offers a rapid method for assessment of the crystallization tendency of amorphous phases. The efficacy of potential crystallization inhibitors can thus be rapidly evaluated. Because of the improved sensitivity, the high-intensity XRD technique becomes useful even if the weight fraction of the analyte in a formulation is low.

CONCLUSIONS

An X-ray diffraction technique was developed using synchrotron X-rays, 2-D detector, and a rapid acquisition system that can provide high-quality powder patterns with a time resolution down to 40 ms. An *in situ* crystallization approach was used to demonstrate the utility of the XRD technique for crystallinity quantification. A novel algorithm was developed for separation of crystalline and amorphous intensity contributions from an X-ray pattern. The crystallinity determination procedure based on this algorithm is objective and requires minimal user intervention. The technique developed is very sensitive to subtle changes in the lattice order of amorphous materials. The estimated LOD for the method is ~0.2% w/w.

ACKNOWLEDGMENTS

This work was made possible by the allocation of beam time at the European Synchrotron Radiation Facility (ESRF), Grenoble, France. We thank Dr. Theyencheri Narayanan, Scientist in Charge, ID2 High Brilliance Beamline, ESRF for his assistance and support. The scientific and technical support provided by Dr. Ramprakash Govindarajan is gratefully acknowledged.

REFERENCES

1. S. Miyazaki, H. Endo, T. Nadai, T. Arita, and M. Nakano. Effect of formulation additives on the dissolution behavior of tetracycline antibiotics. *Chem. Pharm. Bull.* **25**:1186–1193 (1977).
2. H. Imaizumi, N. Nambu, and T. Nagai. Stability and several physical properties of amorphous and crystalline form of indomethacin. *Chem. Pharm. Bull.* **28**:2565–2569 (1980).
3. J. D. Mullins and T. J. Macek. Some pharmaceutical properties of novobiocin. *J. Am. Pharm. Assoc.* **49**:245–248 (1960).
4. K. Tanaka, T. Takeda, and K. Miyajima. Cryoprotective effect of saccharides on denaturation of catalase by freeze-drying. *Chem. Pharm. Bull.* **39**:1091–1094 (1991).
5. K. Izutsu, S. Yoshioka, and T. Terao. Effect of mannitol crystallinity on the stabilization of enzymes during freeze-drying. *Chem. Pharm. Bull.* **42**:5–8 (1994).
6. K. Izutsu, S. Yoshioka, and T. Terao. Decreased protein-stabilizing effects of cryoprotectants due to crystallization. *Pharm. Res.* **10**:1232–1237 (1993).
7. M. Yoshioka, B. C. Hancock, and G. Zografi. Crystallization of indomethacin from the amorphous state below and above its glass transition temperature. *J. Pharm. Sci.* **83**:1700–1705 (1994).
8. International Conference on Harmonisation (ICH). Draft guidance on Q6A specifications: test procedures and acceptance criteria for new drug substances and new drug products: chemical substances. *Fed. Regist.* **65**:83041–83063 (2000).
9. U.S. Department of Health and Human Services, Food and Drug Administration. Process analytical technology—a framework for innovative pharmaceutical manufacturing and quality assurance. Draft guidance. *Fed. Regist.* **68**:52781–52782 (2003).
10. S. Byrn, R. Pfeiffer, M. Ganey, C. Hoiberg, and G. Poochikian. Pharmaceutical solids: a strategic approach to regulatory considerations. *Pharm. Res.* **12**:945–954 (1995).
11. L. S. Taylor and G. Zografi. The quantitative analysis of crystallinity using FT-Raman spectroscopy. *Pharm. Res.* **15**: 755–761 (1998).
12. A. Saleki-Gerhardt, C. Ahlneck, and G. Zografi. Assessment of disorder in crystalline solids. *Int. J. Pharm.* **101**:237–247 (1994).
13. T. Sebhatu, M. Angberg, and C. Ahlneck. Assessment of the degree of disorder in crystalline solids by isothermal microcalorimetry. *Int. J. Pharm.* **104**:135–144 (1994).
14. M. J. Pikal, A. L. Lukes, J. E. Lang, and K. Gaines. Quantitative crystallinity determinations for beta-lactam antibiotics by solution calorimetry: correlations with stability. *J. Pharm. Sci.* **67**: 767–773 (1978).
15. R. Suryanarayanan. X-ray powder diffractometry. In H. G. Brittain (ed.), *Physical Characterization of Pharmaceutical Sciences*, Marcel Dekker, New York, 1995, pp. 187–221.
16. P. H. Hermans and A. Weidinger. Quantitative X-ray investigation on the crystallinity of cellulose fibers. A background analysis. *J. Appl. Phys.* **19**:491–506 (1948).
17. P. H. Hermans and A. Weidinger. Quantitative investigation of X-ray diffraction by "amorphous" polymers and some other noncrystalline substances. *J. Polym. Sci.* **5**:269–281 (1950).

18. R. Surana and R. Suryanarayanan. Quantitation of crystallinity in substantially amorphous pharmaceuticals and study of crystallization kinetics by X-ray powder diffractometry. *Powder Diffr.* **15**:2–6 (2000).
19. A. Saleki-Gerhardt and G. Zografi. Non-isothermal and isothermal crystallization of sucrose from the amorphous state. *Pharm. Res.* **11**:1166–1173 (1994).
20. C. J. Kedward, W. MacNaughtan, and J. R. Mitchell. Isothermal and non-isothermal crystallization in amorphous sucrose and lactose at low moisture contents. *Carbohydr. Res.* **329**:423–430 (2000).
21. B. Makower and W. B. Dye. Equilibrium moisture content and crystallization of amorphous sucrose and glucose. *J. Agric. Food Chem.* **4**:72–77 (1956).
22. K. G. Van Scoik and J. T. Carstensen. Nucleation phenomena in amorphous sucrose systems. *Int. J. Pharm.* **58**:185–196 (1990).
23. A. Mahendrasingam, W. Fuller, V. T. Forsyth, R. J. Oldman, D. MacKerron, and D. J. Blundell. X-ray camera for high- and small-angle X-ray diffraction studies of the drawing and annealing of polymers at Daresbury Synchrotron Radiation Source. *Rev. Sci. Instrum.* **63**:1087–1090 (1992).
24. C. Nunes. *Use of High-Intensity X-Radiation in Solid-State Characterization of Pharmaceuticals*, Ph.D. Dissertation, Department of Pharmaceutics, University of Minnesota, 2005.
25. A. Mahendrasingam, C. Martin, S. Bingham, W. Fuller, and D. J. Blundell. Synchrotron studies of polymers at high spatial and temporal resolution. *Adv. X-ray Anal.* **43**:356–365 (2000).
26. A. Mahendrasingam, D. J. Blundell, A. K. Wright, V. Urban, T. Narayanan, and W. Fuller. Observations of structure development during crystallisation of oriented poly(ethylene terephthalate). *Polymer* **44**:5915–5925 (2003).
27. D. J. Hughes, A. Mahendrasingam, C. Martin, W. B. Oatway, E. L. Heeley, S. J. Bingham, and W. Fuller. An instrument for the collection of simultaneous small and wide angle X-ray scattering and stress–strain data during deformation of polymers at high strain rates using synchrotron radiation sources. *Rev. Sci. Instrum.* **70**:4051–4054 (1999).
28. Powder Diffraction File (PDF-2), International Centre for Diffraction Data, Newtown Square, PA, 1998.
29. G. Zografi. States of water associated with solids. *Drug Dev. Ind. Pharm.* **14**:1905–1926 (1988).
30. M. J. Kontny and G. Zografi. Sorption of water by solids. In H. G. Brittain (ed.), *Physical Characterization of Pharmaceutical Solids*, Marcel Dekker, New York, 1995, pp. 387–418.
31. B. C. Hancock and G. Zografi. Characteristics and significance of the amorphous state in pharmaceutical systems. *J. Pharm. Sci.* **86**:1–12 (1997).
32. G. A. Stephenson, R. A. Forbes, and S. M. Reutzel-Edens. Characterization of the solid state: quantitative issues. *Adv. Drug Deliv. Rev.* **48**:67–90 (2001).
33. D. B. Black and E. G. Lovering. Estimation of the degree of crystallinity in digoxin by X-ray and infrared methods. *J. Pharm. Pharmacol.* **29**:684–687 (1977).
34. A. Galvan-Sanchez, F. Urena-Nunez, H. Flores-Llamas, and R. Lopez-Castanares. Determination of the crystallinity index of iron polymethacrylate. *J. Appl. Polym. Sci.* **74**:995–1002 (1999).
35. S. L. Shamblin, E. Y. Huang, and G. Zografi. The effects of co-lyophilized polymeric additives on the glass transition temperature and crystallization of amorphous sucrose. *J. Therm. Anal.* **47**:1567–1579 (1996).
36. D. A. Skoog and J. J. Leary. *Principles of Instrumental Analysis*, Harcourt Brace College, Forth Worth, TX, 1992.
37. V. Thomsen, D. Schatzlein, and D. Mercuro. Limits of detection in spectroscopy. *Spectroscopy* **18**:112–114 (2003).